

Proceeding Paper

# X-ray Diffraction Study of Fluorine-Functionalized Thiosemicarbazones and Cyclometallated Compounds †

Marcos Rúa-Sueiro \* , Paula Munín-Cruz , Juan M. Ortigueira  and José M. Vila

Department of Inorganic Chemistry, Faculty of Chemistry, University of Santiago de Compostela, Avda. das Ciencias s/n, 15782 Santiago de Compostela, Spain; paula.munin@usc.es (P.M.-C.); juanm.ortigueira@usc.es (J.M.O.); josemanuel.vila@usc.es (J.M.V.)

\* Correspondence: marcos.rua.sueiro@usc.es

† Presented at the 3rd International Online Conference on Crystals, 15–30 January 2022; Available online: [https://iocc\\_2022.sciforum.net/](https://iocc_2022.sciforum.net/).

**Abstract:** In this work, an X-ray diffraction study of fluorine-functionalized thiosemicarbazone ligands and their corresponding cyclometallated compounds is discussed. The results are in agreement with previous characterization by IR spectroscopy,  $^1\text{H}$  and  $^{19}\text{F}$  NMR spectroscopy. Suitable crystals were obtained for a thiosemicarbazone ligand and a cyclometallated compound. The crystal structure analyses are in accordance with the proposed structures: a fluorine-functionalized thiosemicarbazone ligand and a cyclometallated compound in which the thiosemicarbazone is a tridentate [C, N, S] ligand. A comparative study of bond distances and angles is shown, providing information about the coordination of the ligand to the metal center.

**Keywords:** X-ray; thiosemicarbazone; palladium; cyclometallation; fluorine



**Citation:** Rúa-Sueiro, M.; Munín-Cruz, P.; Ortigueira, J.M.; Vila, J.M. X-ray Diffraction Study of Fluorine-Functionalized Thiosemicarbazones and Cyclometallated Compounds. *Chem. Proc.* **2022**, *9*, 3. [https://doi.org/10.3390/IOCC\\_2022-12140](https://doi.org/10.3390/IOCC_2022-12140)

Academic Editor: Ana Garcia-Deibe

Published: 12 January 2022

**Publisher's Note:** MDPI stays neutral with regard to jurisdictional claims in published maps and institutional affiliations.



**Copyright:** © 2022 by the authors. Licensee MDPI, Basel, Switzerland. This article is an open access article distributed under the terms and conditions of the Creative Commons Attribution (CC BY) license (<https://creativecommons.org/licenses/by/4.0/>).

## 1. Introduction

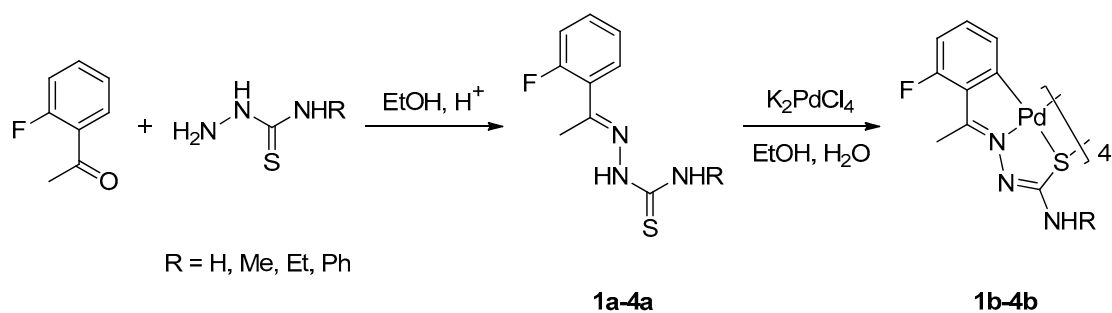
In this work, fluorine-thiosemicarbazone ligands were used to synthesize cyclometallated palladium compounds. The fluorine functionality increases their solubility, which is one of the main issues when dealing with this type of species [1,2].

The ligands are widely used in coordination and organometallic chemistry due to the number of different heteroatoms and their versatile coordination to metal centers [3], generating a wide range of compounds. In addition, these ligands are relevant in the biological field; the free ligands themselves possess a certain degree of biological activity [4,5], usually enhanced by coordination to one or more metal atoms [6,7].

Furthermore, cyclometallated compounds are a large family of complexes that contain a chelate ring comprising a coordinated heteroatom–metal bond or a  $\sigma$  carbon–metal bond [8,9]. The metalated atom may be an aromatic [10,11] or alkenyl [12]  $\text{sp}^2$  carbon or an  $\text{sp}^3$  carbon [13]. Many of these compounds are used in catalysis, and they produce very good results in cross-coupling reactions with carbon–carbon bond formation (Suzuki–Miyaura [14,15] and Mizoroki–Heck [16,17]) and carbon–nitrogen bond formation (Buchwald–Hartwig [18,19]). Likewise, their biological activity has been shown to be quite high, and it has been tested for a huge variety of metals and ligands [20–23].

## 2. Results and Discussion

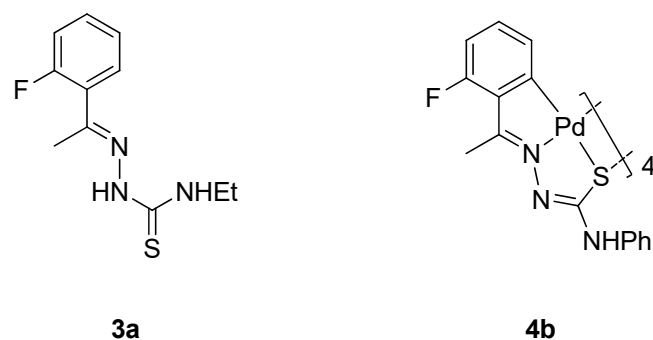
An X-ray diffraction study of a thiosemicarbazone ligand and the ensuing palladium cyclometallated product is discussed (see Scheme 1). The results agree with a previous characterization by IR,  $^1\text{H}$  NMR and  $^{19}\text{F}$  NMR spectroscopies [24]. In addition, a structural study and comparison between the two structures were carried out.



**Scheme 1.** Reaction sequence leading to the synthesis of cyclometallated complexes containing fluor atoms.

### 2.1. X-ray Diffraction Study

Suitable crystals for compounds were obtained by slow evaporation of a DMSO–acetone (**3a**) or chloroform (**4b**) solution, shown in Scheme 2. The X-ray diffraction study showed the proposed structures. The structures were solved by direct methods and refined by full-matrix least-squares on  $F^2$ . Hydrogen atoms were included in calculated positions. Refinement converged at a final  $R_1 = 0.0302$  and  $wR_2 = 0.0712$  (compound **3a**) and  $R_1 = 0.0299$  and  $wR_2 = 0.0625$  (compound **4b**) with allowance for thermal anisotropy of all non-hydrogen atoms. The structure solution and refinement were carried out using the program OLEX2 [25].



**Scheme 2.** Compounds **3a** and **4b** were studied by X-ray diffraction study.

#### 2.1.1. Compound 3a

Compound **3a** crystallizes in a monoclinic system,  $P2_1/n$  space group. The unit cell contains four molecules of thiosemicarbazone (see Figure 1). Crystal data is shown in Appendix A (Table A1).

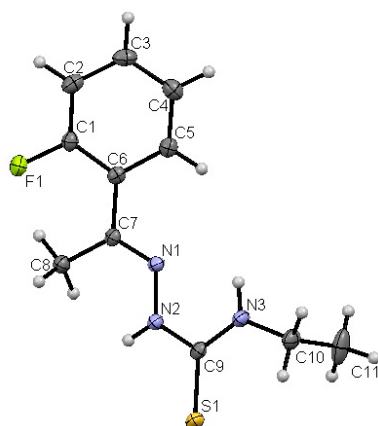


**Figure 1.** Molecular structure of ligand **3a**. Thermal ellipsoids are shown at 50% probability level.

The structure shows thiosemicarbazone in the thionic form, with *E* conformation [26], probably due to the intramolecular interaction (2.179 Å) between the imine nitrogen and the thioamide proton, shown in Figure 2a.

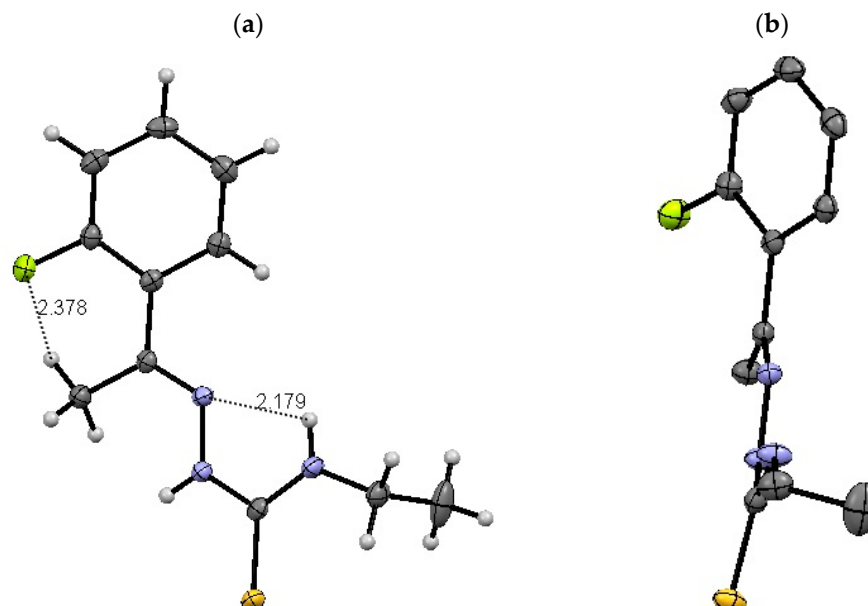


**Figure 2.** (a) Intramolecular interactions between F(1)-H and N(1)-H. (b) Deviation of the phenyl ring from the thiosemicarbazone plane.

In addition, intramolecular interaction (2.378 Å) between the fluorine atom and the imine methyl group is observed. Consequently, in Figure 2b, the aromatic ring is turned away from the thiosemicarbazone plane, with a 34.34° deviation.

### 2.1.2. Compound 4b

Compound **4b** crystallizes in a triclinic system, *P*-1 space group. The unit cell contains two cyclometallated molecules and eight chloroform molecules. Crystal data is shown in Appendix A (Table A2).

The thiosemicarbazone acts as a tridentate ligand (see Figure 3a), generating two five-membered chelate rings, and the compound shows a tetranuclear structure in Figure 3b, with the ligands assuming an antiparallel arrangement and being perpendicular to each other.

In one of the monomers, the palladium center (Pd1) is surrounded by the ortho aromatic carbon of the phenyl ring (C5), the imine nitrogen (N1) and two sulfur atoms (S1 and S2) exhibiting two different bonds with palladium: Pd–S<sub>chelate</sub> (S1) and Pd–S<sub>bridging</sub> (S2).

As in the thiosemicarbazone ligand, an intramolecular interaction of ca. 2.5 Å (Figure 4) is observed between the fluorine atom and the imine methyl group. In this case, the aromatic ring is unable to rotate due to metallation, so the methyl group displays an eclipsed conformation.

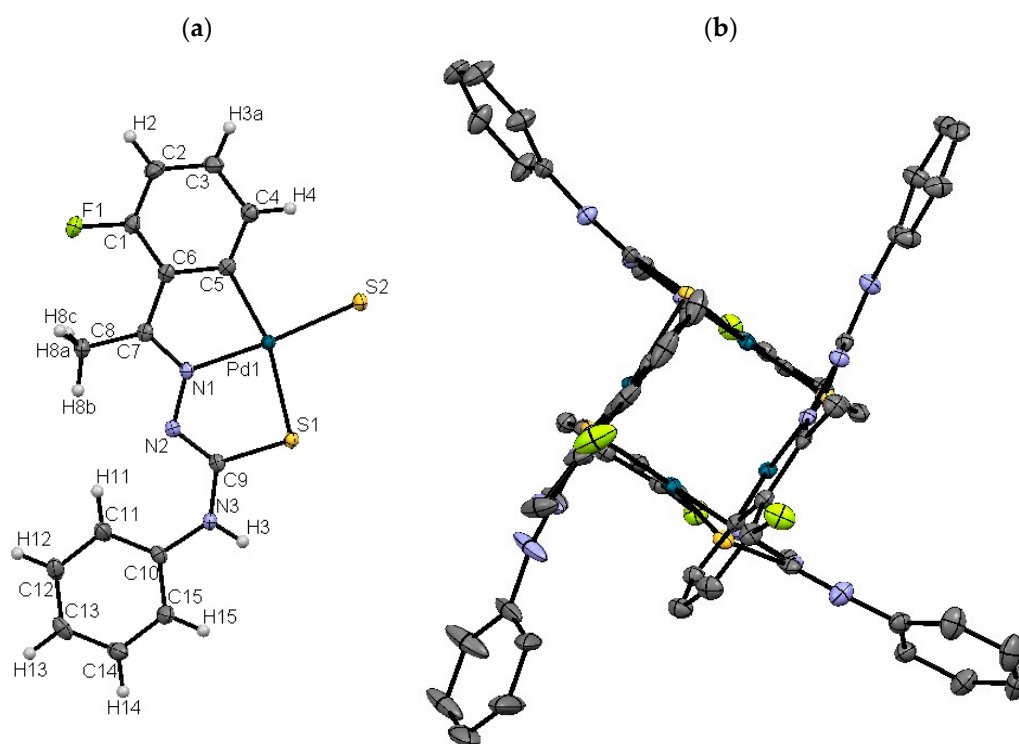


**Figure 3.** (a) Molecular structure of a monomer of **4b**. Thermal ellipsoids are shown at 50% probability level. (b) Molecular structure of **4b**, with antiparallel and perpendicular arrangement of each thiosemicarbazone.

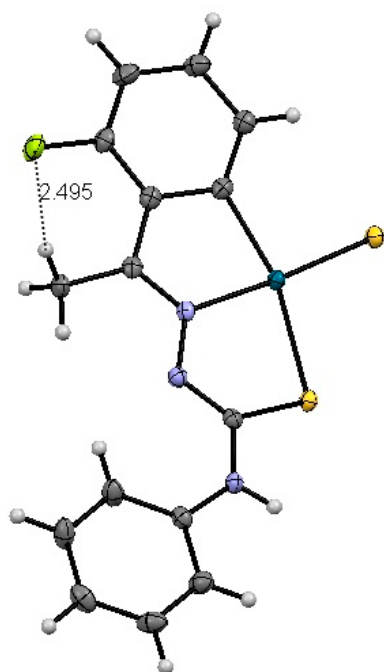


**Figure 4.** Intramolecular interaction of F(1)-H in compound **4b**.

### 2.1.3. Comparison between Bond Distances (Å) and Angles (°)

A comparative study of bond distances (Table 1) and angles (Table 2) between the thiosemicarbazone ligand **3a** and the cyclometallated compound **4b** was carried out.

**Table 1.** Comparison between bonds in compounds **3a** and **4b**.

Bond	3a/Å	4b/Å
N(1)-C(7)	1.2870(18)	1.304(3)
C(9)-N(2)	1.3677(18)	1.297(3)
C(9)-S(1)	1.6816(14)	1.807(3)
C(9)-N(3)	1.3297(18)	1.361(3)
C(5)-C(6)	1.399(2)	1.424(4)

**Table 2.** Comparison between angles in compounds **3a** and **4b**.

Angle	3a/°	4b/°
C(5)-C(6)-C(7)	121.14(12)	116.3(2)
N(1)-N(2)-C(9)	117.90(11)	114.1(2)
N(2)-C(9)-S(1)	119.57(11)	125.16(19)
N(2)-C(9)-N(3)	115.62(12)	120.6(2)
N(3)-C(9)-S(1)	124.81(11)	114.08(18)

The N(1)-C(7) and C(5)-C(6) bonds are somewhat longer in the cyclometallated compound due to the back-bonding of the palladium metal to the N(1) and the C(5) atoms, respectively.

The C(9)-N(2) and C(9)-S(1) bond differences are because of metallation; since it occurs in the thiolic form of the thiosemicarbazone, tautomerization of the C(9)=S(1) double bond is thus needed.

The C(9)-N(3) bond is slightly longer, probably due to the tautomerization of the thionic bond and the coordination of the sulfur atom.

The N(2)-C(9)-S(1), N(2)-C(9)-N(3) and N(3)-C(9)-S(1) angles change upon going to the cyclometallated compound due to the tautomerization and the coordination of the sulfur atom to palladium.

The C(5)-C(6)-C(7) and N(1)-N(2)-C(9) are smaller due to the formation of the five-membered chelate ring upon cyclometallation.

#### 2.1.4. Palladium Bonds and Angles in Compound **4b**

The bond distances with palladium are in accordance with those found in similar complexes [27–29] and angles with a square-planar geometry of the metal center (see Table 3).

**Table 3.** Distance bonds (Å) and angles (°) around palladium metal center.

Bond	/Å	Angle	/°
Pd(1)-N(1)	1.996(2)	N(1)-Pd(1)-C(5)	81.24(9)
Pd(1)-C(5)	2.003(2)	N(1)-Pd(1)-S(1)	83.31(6)
Pd(1)-S(2)	2.3060(6)	C(5)-Pd(1)-S(2)	94.39(8)
Pd(1)-S(1)	2.3729(6)	S(2)-Pd(1)-S(1)	100.81(2)
		N(1)-Pd(1)-S(2)	174.68(6)
		C(5)-Pd(1)-S(1)	164.07(8)

### 3. Conclusions

- X-ray structural analysis was carried out for a thiosemicarbazone ligand and its cyclometallated palladium derivative.
- A comparative study allowed the determination of variations in bond distances and angles in the structure of the ligand after the cyclometallation process.
- The metal atom displays the typical square-planar geometry for palladium.

**Author Contributions:** Conceptualization, M.R.-S. and P.M.-C.; methodology, M.R.-S.; software, M.R.-S.; validation, M.R.-S. and P.M.-C.; formal analysis, M.R.-S.; investigation, M.R.-S. and P.M.-C.; resources, J.M.O. and J.M.V.; data curation, M.R.-S. and P.M.-C.; writing—original draft preparation, M.R.-S.; writing—review and editing, M.R.-S.; visualization, M.R.-S. and P.M.-C.; supervision, J.M.O. and J.M.V.; project administration, M.R.-S. and J.M.V.; funding acquisition, J.M.O. and J.M.V. All authors have read and agreed to the published version of the manuscript.

**Funding:** This research was funded by Xunta de Galicia (Galicia, Spain) under the Grupos de Referencia program (GRC 2019/014).

**Conflicts of Interest:** The authors declare no conflict of interest.

## Appendix A

**Table A1.** Crystal data and structure refinement for **3a**.

Identification code	<b>3a</b>
Empirical formula	C <sub>11</sub> H <sub>14</sub> FN <sub>3</sub> S
Formula weight	239.31
Temperature	100(2) K
Wavelength	0.71073 Å
Crystal system	Monoclinic
Space group	P2 <sub>1</sub> /n
Unit cell dimensions	a = 5.8663(2) Å, α = 90° b = 19.5573(6) Å, β = 105.0047(10)°. c = 10.5485(3) Å, γ = 90°.
Volume	1168.96(6) Å <sup>3</sup>
Z	4
Density (calculated)	1.360 Mg/m <sup>3</sup>
Absorption coefficient	0.266 mm <sup>-1</sup>
F(000)	504
Crystal size	0.240 × 0.127 × 0.119 mm <sup>3</sup>
Theta range for data collection	2.083 to 26.366°.
Index ranges	−6 ≤ h ≤ 7, −24 ≤ k ≤ 24, −13 ≤ l ≤ 13
Reflections collected	32894
Independent reflections	2399 [R(int) = 0.0527]
Completeness to theta = 25.242°	100.0%
Refinement method	Full-matrix least-squares on F <sup>2</sup>
Data/restraints/parameters	2399/0/147
Goodness-of-fit on F <sup>2</sup>	1.050
Final R indices [I > 2σ(I)]	R <sub>1</sub> = 0.0302, wR <sub>2</sub> = 0.0712
R indices (all data)	R <sub>1</sub> = 0.0372, wR <sub>2</sub> = 0.0751
Largest diff. peak and hole	0.246 and −0.266 e·Å <sup>-3</sup>

**Table A2.** Crystal data and structure refinement for **4b**.

Identification code	<b>4b</b>
Empirical formula	C <sub>64</sub> H <sub>52</sub> Cl <sub>12</sub> F <sub>4</sub> N <sub>12</sub> Pd <sub>4</sub> S <sub>4</sub>
Formula weight	2044.41
Temperature	100(2) K
Wavelength	0.71073 Å
Crystal system	Triclinic
Space group	P-1
Unit cell dimensions	a = 13.6814(4) Å, α = 87.1620(10)° b = 15.1512(4) Å, β = 79.4790(10)° c = 19.9092(5) Å, γ = 64.1110(10)°
Volume	3648.25(17) Å <sup>3</sup>
Z	2
Density (calculated)	1.861 Mg/m <sup>3</sup>
Absorption coefficient	1.585 mm <sup>-1</sup>
F(000)	2016
Crystal size	0.180 × 0.160 × 0.070 mm <sup>3</sup>
Theta range for data collection	2.082 to 28.342°.
Index ranges	−18 ≤ h ≤ 18, −20 ≤ k ≤ 20, −26 ≤ l ≤ 26
Reflections collected	112138
Independent reflections	18195 [R(int) = 0.0390]
Completeness to theta = 25.242°	99.9%
Refinement method	Full-matrix least-squares on F <sup>2</sup>
Data/restraints/parameters	18195/0/1020
Goodness-of-fit on F <sup>2</sup>	1.049
Final R indices [I>2sigma(I)]	R <sub>1</sub> = 0.0299, wR <sub>2</sub> = 0.0625
R indices (all data)	R <sub>1</sub> = 0.0390, wR <sub>2</sub> = 0.0666
Largest diff. peak and hole	2.352 and −1.613 e·Å <sup>-3</sup>

## References

- Abás, E.; Gómez-Bachiller, M.; Colom, E.; Pardina, E.; Rodríguez-Diéguez, A.; Grasa, L.; Laguna, M. Cyclometallated gold(III) complexes against colon cancer. X-ray structure of [Au(C,NPhenylpyridine)(OAc)<sub>2</sub>]. *J. Organomet. Chem.* **2020**, *920*, 121340. [[CrossRef](#)]
- Tong, X.; Zhang, L.; Li, L.; Li, Y.; Yang, Z.; Zhu, D.; Xie, Z. Water-soluble cyclometalated Ir (III) complexes as carrier-free and pure nanoparticle photosensitizers for photodynamic therapy and cell imaging. *Dalton Trans.* **2020**, *49*, 11493–11497. [[CrossRef](#)] [[PubMed](#)]
- Lobana, T.S.; Sharma, R.; Bawa, G.; Khanna, S. Bonding and structure trends of thiosemicarbazone derivatives of metals—An overview. *Coord. Chem. Rev.* **2009**, *253*, 977–1055. [[CrossRef](#)]
- Srishaillam, K.; Ramaiah, K.; Reddy, K.L.; Reddy, B.V.; Rao, G.R. Synthesis and evaluation of molecular structure from torsional scans, study of molecular characteristics using spectroscopic and dft methods of some thiosemicarbazones, and investigation of their anticancer activity. *Chem. Pap.* **2021**, *75*, 3635–3647. [[CrossRef](#)]
- Mrozek-Wilczkiewicz, A.; Malarz, K.; Rejmund, M.; Polanski, J.; Musiol, R. Anticancer activity of the thiosemicarbazones that are based on di-2-pyridine ketone and quinoline moiety. *Eur. J. Med. Chem.* **2019**, *171*, 180–194. [[CrossRef](#)]
- Yousef, T.A.; Abu El-Reash, G.M. Synthesis, and biological evaluation of complexes based on thiosemicarbazone ligand. *J. Mol. Struct.* **2020**, *1201*, 127180. [[CrossRef](#)]
- Özerkan, D.; Ertik, O.; Kaya, B.; Kuruca, S.E.; Yanardag, R.; Ülküseven, B. Novel palladium (II) complexes with tetradentate thiosemicarbazones. Synthesis, characterization, in vitro cytotoxicity and xanthine oxidase inhibition. *Investig. New Drugs* **2019**, *37*, 1187–1197. [[CrossRef](#)]

8. Zaera, F. An organometallic guide to the chemistry of hydrocarbon moieties on transition metal surfaces. *Chem. Rev.* **1995**, *95*, 2651–2693. [[CrossRef](#)]
9. Jain, V.K. Cyclometalated group-16 compounds of palladium and platinum: Challenges and opportunities. *Coord. Chem. Rev.* **2021**, *427*, 213546. [[CrossRef](#)]
10. Munín-Cruz, P.; Reigosa, F.; Rúa-Sueiro, M.; Ortigueira, J.M.; Pereira, M.T.; Vila, J.M. Chemistry of tetradentate [C,N: C,N] iminophosphorane palladacycles: Preparation, reactivity and theoretical calculations. *ChemistryOpen* **2020**, *9*, 1190–1194. [[CrossRef](#)]
11. Lucio-Martínez, F.; Bermúdez, B.; Ortigueira, J.M.; Adams, H.; Fernández, A.; Pereira, M.T.; Vila, J.M. A highly effective strategy for encapsulating potassium cations in small crown ether rings on a dinuclear palladium complex. *Chem.—Eur. J.* **2017**, *23*, 6255–6258. [[CrossRef](#)] [[PubMed](#)]
12. Meng, K.; Li, T.; Yu, C.; Shen, C.; Zhang, J.; Zhong, G. Geminal group-directed olefinic CH functionalization via four-to eight-membered exo-metalloacycles. *Nat. Commun.* **2019**, *10*, 5109. [[CrossRef](#)] [[PubMed](#)]
13. Liu, H.-J.; Ziegler, M.S.; Tilley, T.D. Synthesis, structures, and reactivity studies of cyclometalated N-heterocyclic carbene complexes of ruthenium. *Dalton Trans.* **2018**, *47*, 12138–12146. [[CrossRef](#)] [[PubMed](#)]
14. Samiee, S.; Shiralinia, A.; Hoveizi, E.; Gable, R.W. A new family of oxime palladacycles mixed with unsymmetrical phosphorus ylides; synthesis, structural, cytotoxicity and catalytic activity studies. *J. Organomet. Chem.* **2019**, *900*, 120927. [[CrossRef](#)]
15. Dharani, S.; Kalaiarasi, G.; Sindhuja, D.; Lynch, V.M.; Shankar, R.; Karvembu, R.; Prabhakaran, R. Tetranuclear palladacycles of 3-Acetyl-7-methoxy-2H-chromen-2-one derived Schiff Bases: Efficient catalysts for Suzuki–Miyaura coupling in an aqueous medium. *Inorg. Chem.* **2019**, *58*, 8045–8055. [[CrossRef](#)]
16. López-Mosquera, C.; Grabulosa, A.; Rocamora, M.; Font-Bardia, M.; Muller, G. Cyclopalladated compounds with polyhalogenated benzylphosphanes for the Mizoroki–Heck reaction. *Eur. J. Inorg. Chem.* **2020**, *2020*, 2470–2484. [[CrossRef](#)]
17. Maji, A.; Singh, O.; Singh, S.; Mohanty, A.; Maji, P.K.; Ghosh, K. Palladium-based catalysts supported by unsymmetrical XYZ–1 type pincer ligands: C5 arylation of imidazoles and synthesis of octinoxate utilizing the Mizoroki–Heck reaction. *Eur. J. Inorg. Chem.* **2020**, *2020*, 1596–1611. [[CrossRef](#)]
18. Serrano, J.L.; Girase, T.R. Palladacycles as efficient precatalysts for Negishi and Buchwald–Hartwig amination reactions. In *Palladacycles*; Elsevier: Amsterdam, The Netherlands, 2019; pp. 175–224.
19. Yu, F.; Shen, W.; Sun, Y.; Liao, Y.; Jin, S.; Lu, X.; He, R.; Zhong, L.; Zhong, G.; Zhang, J. Ruthenium-catalyzed C–H amination of aroylsilanes. *Org. Biomol. Chem.* **2021**, *19*, 6313–6321. [[CrossRef](#)]
20. Pike, S.; Lord, R.; Kergreis, A. Influence of ligand and nuclearity on the cytotoxicity of cyclometallated C<sup>∞</sup>N<sup>∞</sup>C platinum (II) complexes. *Chem.—Eur. J.* **2020**, *26*, 14938–14946.
21. Oliveira, C.G.; Romero-Canelón, I.; Coverdale, J.P.; Maia, P.I.S.; Clarkson, G.J.; Deflon, V.M.; Sadler, P.J. Novel tetranuclear Pd II and Pt II anticancer complexes derived from pyrene thiosemicarbazones. *Dalton Trans.* **2020**, *49*, 9595–9604. [[CrossRef](#)]
22. Licona, C.; Delhorme, J.-B.; Riegel, G.; Vidimar, V.; Cerón-Camacho, R.; Boff, B.; Venkatasamy, A.; Tomasetto, C.; Gomes, P.d.S.F.C.; Rognan, D. Anticancer activity of ruthenium and osmium cyclometalated compounds: Identification of ABCB1 and EGFR as resistance mechanisms. *Inorg. Chem. Front.* **2020**, *7*, 678–688. [[CrossRef](#)]
23. Williams, M.R.; Bertrand, B.; Hughes, D.L.; Waller, Z.A.; Schmidt, C.; Ott, I.; O’Connell, M.; Searcey, M.; Bochmann, M. Cyclometallated Au (III) dithiocarbamate complexes: Synthesis, anticancer evaluation and mechanistic studies. *Metallomics* **2018**, *10*, 1655–1666. [[CrossRef](#)] [[PubMed](#)]
24. Rúa Sueiro, M.; Ortigueira, J.M.; Vila, J.M. Cyclometallated thiosemicarbazones containing fluorine atoms: A solubility improvement. In *Proceedings of the 25th International Electronic Conference on Synthetic Organic Chemistry*; MDPI: Basel, Switzerland, 2021.
25. Dolomanov, O.V.; Bourhis, L.J.; Gildea, R.J.; Howard, J.A.; Puschmann, H. Olex2: A complete structure solution, refinement and analysis program. *J. Appl. Crystallogr.* **2009**, *42*, 339–341. [[CrossRef](#)]
26. Casas, J.; Garcia-Tasende, M.; Sordo, J. Main group metal complexes of semicarbazones and thiosemicarbazones. A structural review. *Coord. Chem. Rev.* **2000**, *209*, 197–261. [[CrossRef](#)]
27. Rúa-Sueiro, M.; Munín-Cruz, P.; Reigosa, F.; Vila, J.M.; Ortigueira, J.M. Synthesis and X-Ray diffraction study of thiosemicarbazone palladacycles with dppm. *Proceedings* **2020**, *62*, 13.
28. Martínez, J.; Cabaleiro-Lago, E.M.; Ortigueira, J.M.; Pereira, M.T.; Friero, P.; Lucio, F.; Vila, J.M. Synthesis and reactivity of thiosemicarbazone palladacycles. Crystal structure analysis and theoretical calculations. *Inorg. Chim. Acta* **2016**, *449*, 20–30. [[CrossRef](#)]
29. Pereira, M.T.; Antelo, J.M.; Adrio, L.A.; Martinez, J.; Ortigueira, J.M.; Lopez-Torres, M.; Vila, J.M. Novel bidentate [N,S] palladacycle metalloligands. 1H-15N HMBC as a decisive NMR technique for the structural characterization of Palladium–Rhodium and Palladium–Palladium bimetallic complexes. *Organometallics* **2014**, *33*, 3265–3274. [[CrossRef](#)]